Salt Complexation in Block Copolymer Thin Films

Seung Hyun Kim,[†] Matthew J. Misner,[‡] Ling Yang,[‡] Oleg Gang,[§] Benjamin M. Ocko,[§] and Thomas P. Russell*,[‡]

Division of Nano-Systems Engineering, Inha University, Incheon, South Korea; Department of Polymer Science and Engineering, University of Massachusetts, Amherst, Massachusetts 01003; and Condensed Matter Physics and Materials Science Department, Brookhaven National Lab, Upton, New York 11973

Received May 24, 2006; Revised Manuscript Received July 13, 2006

ABSTRACT: Ion complexation within cylinder-forming block copolymer thin films was found to affect the ordering process of the copolymer films during solvent annealing, significantly enhancing the long-range positional order. Small amounts of alkali halide or metal salts were added to PS-*b*-PEO, on the order of a few ions per chain, where the salt complexed with the PEO block. The orientation of the cylindrical microdomains strongly depended on the salt concentration and the ability of the ions to complex with PEO. The process shows large flexibility in the choice of salt used, including gold or cobalt salts, whereby well-organized patterns of nanoparticles can be generated inside the copolymer microdomains. By further increasing the amount of added salts, the copolymer remained highly ordered at large degrees of swelling and demonstrated long-range positional correlations of the microdomains in the swollen state, which holds promise as a route to addressable media.

Introduction

The self-assembly of block copolymers provides a versatile platform for the fabrication of nanostructured materials. Scaffolds and templates produced from oriented morphologies of block copolymers have been used in applications ranging from filters with well-defined pore sizes for the separation of viruses to floating gates in flash memory storage devices.[1−16] Yet, to utilize fully the areal density of elements afforded by block copolymers and to realize the potential of generating addressable media, control over the orientation and long-range lateral ordering of the copolymer microdomains is necessary. While external fields, such as applied electrical fields or controlled interfacial interactions, provide control over the orientation of the microdomain morphology,[6,9,24,25] producing morphologies with long-range lateral order requires fields in two orthogonal directions. These fields may be either applied, as in the case of an electric field, or there may exist an internal driving force, such as a defect energy in packing, that promotes lateral order.[16−27] In the case of defects, the higher the energetic penalty associated with the presence of the defect, the greater will be the driving force to remove defects and produce long-range lateral order.

Polymer/salt complexes have received considerable attention since they exhibit high ionic conductivity, stable electrochemical characteristics, and excellent mechanical properties.[28−35] In polymer-based electrochemical technologies these complexes are used in solid-state lithium batteries, fuel cells, chemical sensors, and flexible displays. In addition, metal-precursor salts can be confined within the nanoscopic microdomains of the block copolymers, and through subsequent reduction reactions, the precursor salts can be converted to the corresponding metal, providing a simple route for the generation of metallic nanoparticles within the minor component phase of the block copolymer.[36−39] Here, we show that the complexation of alkali halide or metal salts with the poly(ethylene oxide) (PEO) block of a polystyrene (PS)-*block*-PEO copolymer, having cylindrical microdomains of PEO, produces a dramatic, unexpected result during solvent annealing, wherein the microdomains of the block copolymer are found to orient normal to the surface of the film with markedly enhanced lateral order, in comparison to the same films prepared in the absence of salt.

Experimental Section

Commercially available polystyrene-*block*-poly(ethylene oxide) diblock copolymer, PS-*b*-PEO, with a molecular weight of 25.3 kg/mol and a PS weight fraction of 0.75 (corresponding to a volume fraction of 0.76) was used in this study. In the bulk, this asymmetric diblock copolymer self-assembles into hexagonally packed arrays of cylindrical microdomains with diameters of 21 nm with a mean separation of ∼32 nm. Solutions of the block copolymer with and without added salts were spin-coated onto cleaned silicon substrates where the film thickness was controlled by the spinning rate and/or the solution concentration. Salt was added to the copolymer by dissolving the copolymer in tertrahydrofuran and the salt in methanol. Equal volumes of these two solutions were then mixed. After 8−12 h, the copolymer was precipitated by the addition of hexane. The precipitate was then dried and redissolved into benzene. Spin-coated films were placed in a benzene-saturated chamber at room temperature, allowing the benzene vapors to swell the film and solvent-anneal the morphology, as described previously.[27] All solvent-annealing experiments were performed in a chamber where the relative humidity was controlled between 40 and 60%. SFM images were obtained in both the height and phase contrast modes using a Digital Instruments Dimension 3000 scanning force microscope in tapping mode. Transmission electron microscopy (TEM) studies were performed on a JEOL 100CX electron microscope operated at 100 kV. For TEM, the samples were prepared on silicon substrates with a thick layer of silicon oxide. The polymer film was then floated onto the surface of an aqueous solution containing 5 wt % HF, transferred to a water bath, and then retrieved with a Cu grid for measurement. Grazing incident angle small-angle X-ray scattering (GISAXS) measurements were performed at the X22B beamline at the National Synchrotron Light Source (Brookhaven National Laboratory) and at the G1 beamline at CHESS (Cornell University).

Results and Discussion

Previously, we demonstrated that solvent annealing produced a high degree of long-range lateral order of cylindrical micro-

[†] Inha University.
[‡] University of Massachusetts.
[§] Brookhaven National Lab.

10.1021/ma061170k CCC: $33.50
Published on Web 10/25/2006

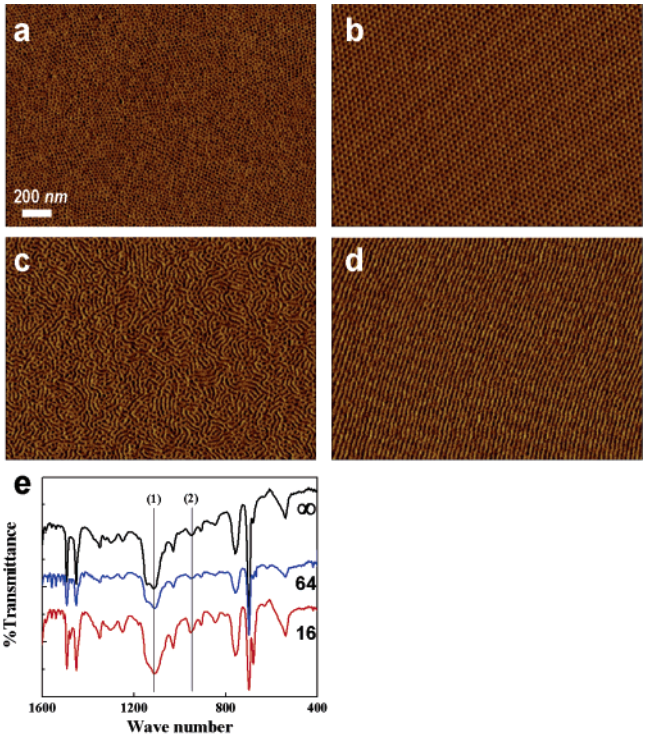

Figure 1. SFM images of block copolymer films containing KI (a) as spun and (b) after solvent annealing and copolymer films without added KI (c) as spun and (d) after solvent annealing. Shifts in the IR spectroscopy of the copolymer with varying monomer-to-salt ratios ([O]/[K]) indicate complexation of the salt with the PEO.

domains, oriented normal to the surface, in thin films of PS-*b*-PEO.[27] More recently, we found that the ordering behavior of PS-*b*-PEO during solvent annealing was highly dependent on the amount of residual salt remaining in the block copolymer from the initiator during synthesis. To investigate the effect of salt concentration on the ordering behavior in block copolymer thin films, controlled amounts of salt were added to PS-*b*-PEO prior to solution casting. Because of the limited solubility of the salts in apolar solvents, the salt and block copolymer were first dissolved in methanol and tetrahydrofuran, respectively, and then mixed together. Subsequently, the block copolymer/salt complexes were precipitated in hexane, redissolved in benzene, and then spin-coated onto silicon wafers. Parts a and b of Figure 1 show the SFM images of thin films of the block copolymer complexed with KI, with a molar ratio of the oxygen in PEO to the cation of the salt of 64 ([O]/[K]), before and after solvent annealing, respectively. The results for films of the block copolymer without salt are shown in parts c and d of Figure 1, respectively. It is clear that the addition of salt gives rise to a change in the orientation of PEO cylinders, from parallel to perpendicular, in the solvent annealed films. The as-spun films exhibit a similar change in the orientation of the cylindrical microdomains from a mixed orientation to an orientation normal to the surface, with and without salt, respectively. Being that the PEO is water-soluble and the salts used are fairly hydroscopic, humidity can affect behavior of block copolymer ordering. Subsequently, the experiments presented here were performed in a controlled humidity environment between 40% and 60%. The complexation of KI with the PEO block is further demonstrated by infrared (IR) spectroscopy. Here the positions of the C−O−C (1) stretching and CH_2 (2) rocking modes in PEO were shifted in comparison to the salt-free polymer film. Figure 1e illustrates that the positions are slightly shifted from 1113 to 1111 cm^{-1} to 1109 and 947 cm^{-1} to 949 to 953 cm^{-1}, as the concentration was increased from [O/K] = ∞ to 64 to 16, respectively.

Large differences in the evolution of structure upon solvent annealing were observed by in-situ GISAXS for films with different salt concentrations. By exposing the film to a solvent environment the copolymer film is rapidly swollen and, as the solvent atmosphere is depleted, the solvent evaporates from the copolymer film. For the block copolymer with small to medium amounts of added salts, the copolymer film disorders upon swelling and produces a highly ordered array of hexagonally packed cylindrical microdomains oriented normal to the surface of the film when the solvent is removed. Figure 2 shows two GISAXS patterns, where the angle of incidence was above the critical angle of the polymer and full penetration of the X-ray beam into the film occurred. In Figure 2a, the copolymer film contained a small amount of salt ([O]/[K] = 64) and was swollen to ~250% of the original film thickness. Only diffuse surface scattering was observed, indicating that the copolymer was disordered. It is clear from the scattering pattern from the swollen copolymer film without salt (Figure 2b) that some order is still present inside the film. This result underscores the significance of preferential interactions of the PEO block of the copolymer with the silicon oxide substrate. Below the critical angle, where the penetration of the X-ray beam extends only a few nanometers into the film, only diffuse scattering was observed, indicating that the copolymer was disordered at the

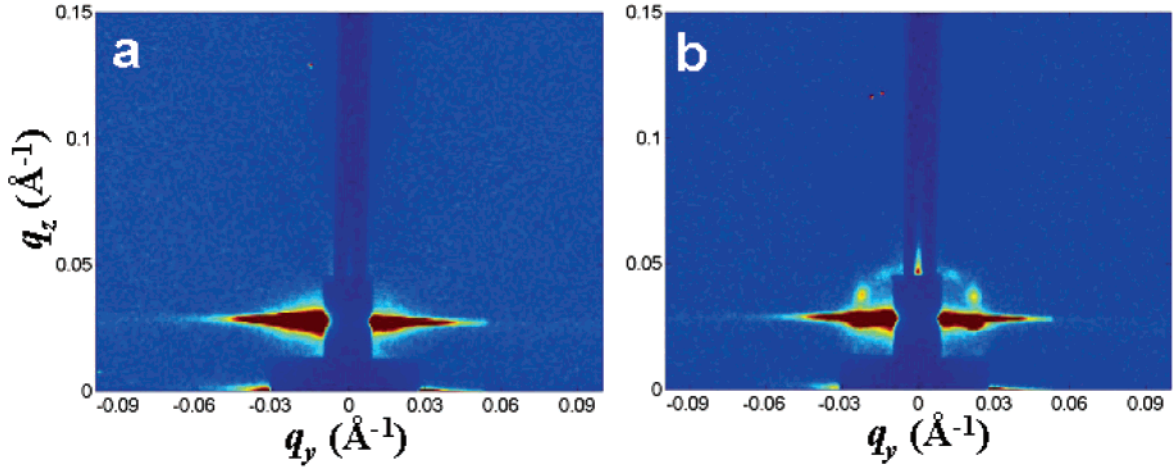

Figure 2. GISAXS patterns of swollen copolymer films (a) with and (b) without a small amount of salt added, where the salts can screen favorable interactions with the substrate, where otherwise the film is completely disordered.

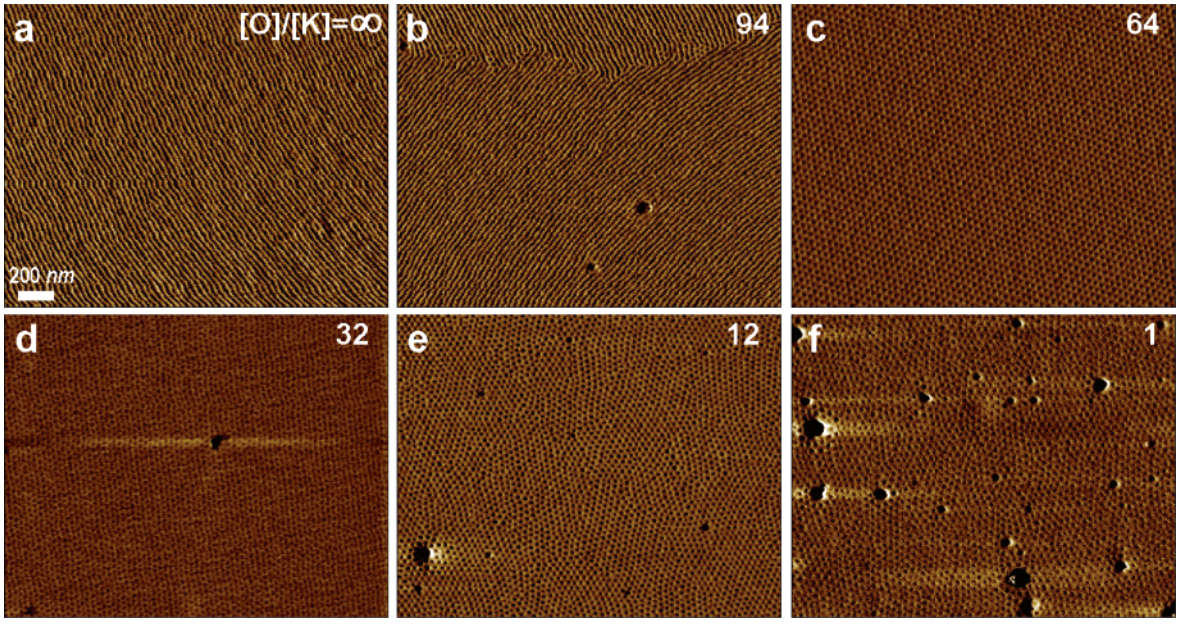

Figure 3. SFM images of copolymer films containing different amounts of added salt from no added salt to a ratio of oxygen in the PEO to the number ions of unity. Increasing the salt concentration can induce a change of microdomain orientation in the copolymer film.

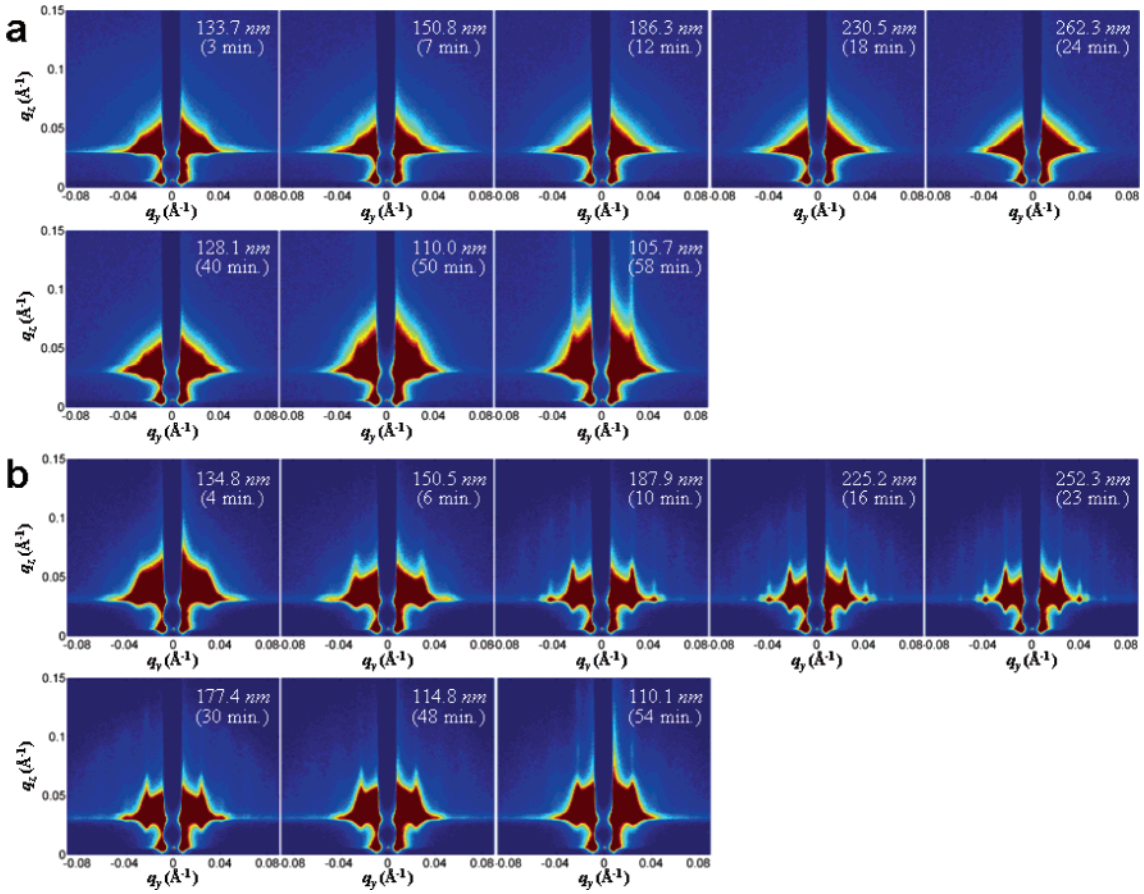

Figure 4. Series of in-situ GISAXS patterns at (a) 64 ([O]/[K]) and (b) 16 ([O]/[K]), where the top row of each series is while the copolymer film is swelling and the bottom row of each series is while solvent is evaporating from the copolymer film. The copolymer film with a low salt concentration quickly disorders on swelling and then reorders during evaporation of the solvent, while the film with a high salt concentration never disorders and demonstrates an extremely correlated structure in the swollen state. This correlation is lost upon evaporation of the solvent.

free surface. Without the addition of salt to the block copolymer, as the solvent evaporates, the cylindrical microdomains form a hexagonally packed array of cylinders oriented parallel to the films surface. Together these results indicate that the salt, either by complexation with the PEO or by interactions with the substrate, overcomes preferential interactions between the PEO and the substrate, enabling the propagation of a front of ordered cylindrical microdomains through the film oriented normal to the film surface.

The SFM images shown in Figure 3 show the dependence of the orientation and the lateral order of the block copolymer microdomains in thin films on the salt concentration. At a low

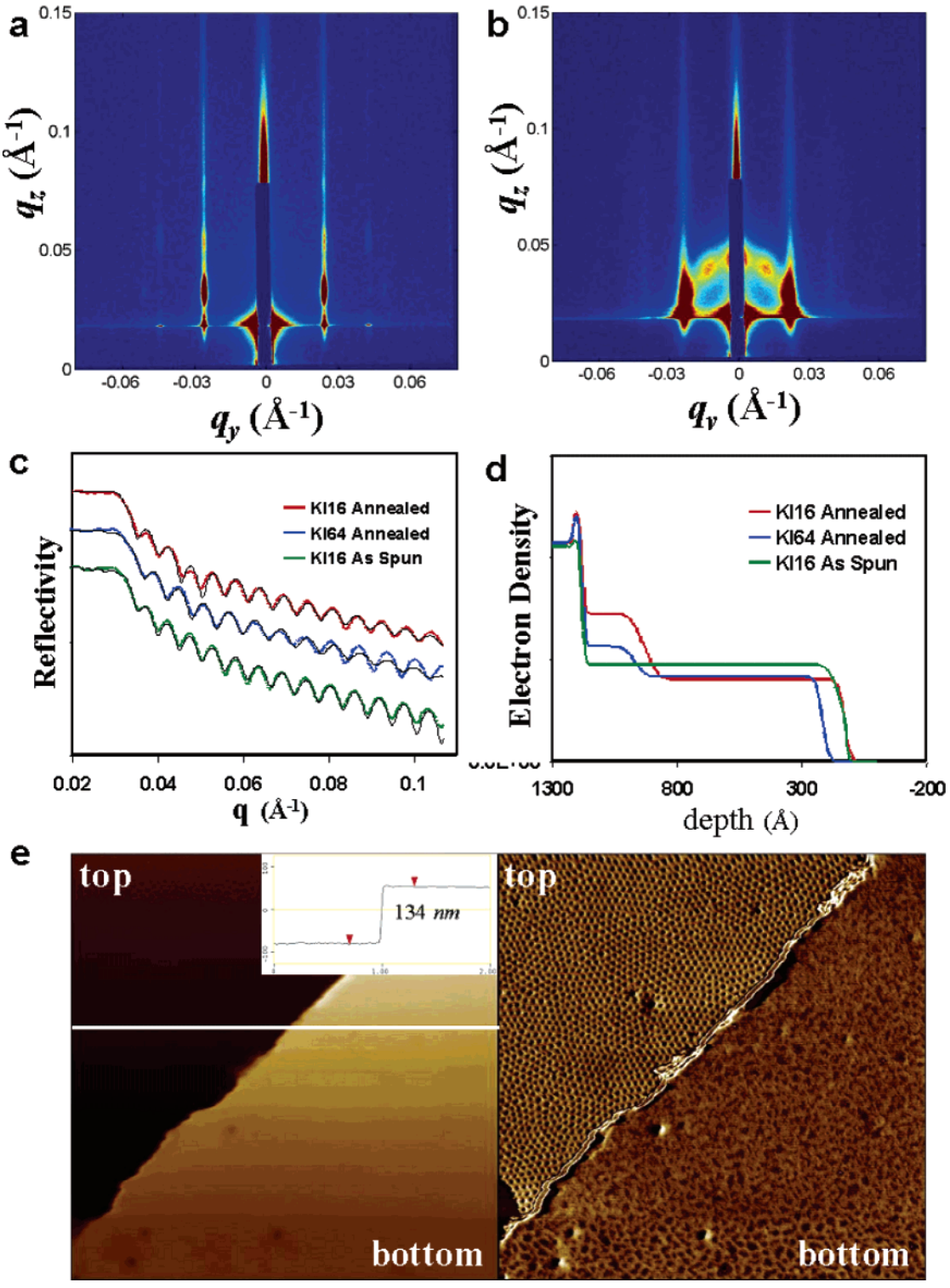

Figure 5. Static GISAXS patterns with salt concentrations of (a) 64 ([O]/[K]) and (b) 16 ([O]/[K]). Additional reflections are observed in the film with higher salt concentration that are not observed in the film with lower salt concentration. X-ray reflectivity profiles (c) and the fitted electron density profiles (d) indicate that the salt is distributed near the substrate. (e) 2 × 2 μm SFM height and phase images of a film that has been removed from the substrate and flipped back onto itself such that the top and bottom of the film are exposed. The structure at the bottom of the film is similar to, but different from, the top of the film.

concentration of salt ([O]/[K] = 94), the amount of added salt is insufficient to overcome the strong interfacial interactions, and the microdomains orient parallel to the surface. With increasing the salt concentrations ([O]/[K] = 64 and 32), highly ordered arrays of cylindrical microdomains oriented normal to the surface are observed. Increasing the salt concentration further ([O]/[K] = 12) maintains the orientation of the microdomains normal to the surface; however, the lateral ordering of the cylindrical microdomains is reduced.

To explore the details of the solvent annealing process, in-situ GISAXS measurements were performed in real time.[40,41] Simultaneously, the film thickness was measured by multi-wavelength optical interferometry to assess the concentration of solvent in the film. Sequences of GISAXS patterns are shown

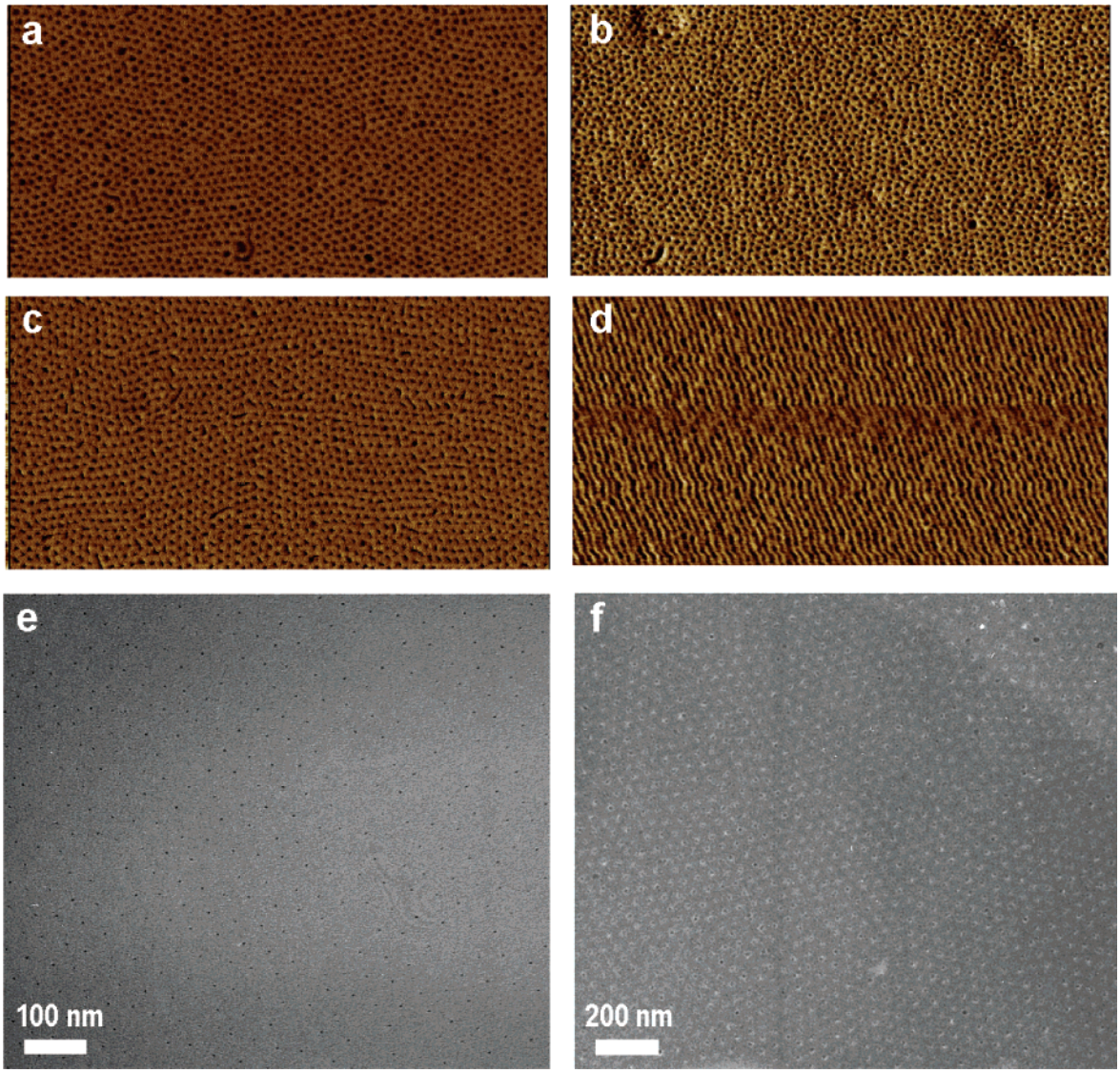

Figure 6. Salts that can complex with PEO all show similar results, including (a) LiI, (b) RbI, and (c) LiCl; however, (d) KCl does not complex and does not induce microdomain reorientation, as seen in the 2 × 1 μm SFM images. Through the complexation of (e) gold and (f) cobalt salts nanoparticles can be generated inside the copolymer microdomains.

in Figure 4a for [O]/[K] = 64 and Figure 4b for [O]/[K] = 16 during the swelling of the copolymer film such that the final film thickness is more than twice the thickness of the original film and during the deswelling at room temperature. In each series the top row corresponds to the swelling of the film, while the bottom row in the series corresponds to solvent removal. The time from the addition of solvent ($t = 0$) and film thickness at that time are specified in each figure. The Bragg rods (vertical streaks) in the GISAXS patterns correspond to the first-order reflection from a 2D hexagonal lattice of cylinders of finite length oriented normal to the surface. At the lower salt concentration ([O]/[K] = 64), the copolymer rapidly disordered and underwent microphase separation near the end of solvent evaporation, as discussed above. However, for the sample with the higher salt concentration ([O]/[K] = 16), the copolymer remained microphase separated throughout the swelling, and in fact, the lateral ordering and in-plane correlations markedly improved. Many higher-order reflections were observed at scattering vectors characteristic of hexagonally close-packed cylindrical microdomains oriented normal to the film surface. Upon removal of the solvent the higher-order reflections in the GISAXS are lost, even though the films show exceptional lateral ordering by SFM over areas tens of square microns in size. That the film remains ordered and the spacing between the microdomains increases during swelling indicates that complexation of the PEO with the salt has increased the effective segmental interactions between the PS and PEO. The increased nonfavorable interactions, coupled with the enhanced mobility of the polymer chains in the highly swollen film, give rise to the exceptional degree of lateral ordering in the film seen in the GISAXS experiment. Unfortunately, as the solvent evaporates, the volume change in the film coupled with the lateral confinement to the substrate results in a loss of lateral order within the film (not observable by SFM). Experiments are in progress to develop systems where the block copolymer can be cross-linked in the swollen state, thereby locking in the highly ordered, oriented cylindrical microdomain morphology.

Parts a and b of Figure 5 show static GISAXS patterns of copolymer films after solvent annealing with salt concentrations of [O]/[K] = 64 and [O]/[K] = 16, respectively. Strong vertical streaks in both films indicate the presence of cylindrical microdomains oriented normal to the surface. However, with the higher salt concentration there are additional reflections in the GISAXS pattern at an in-plane wave-vector at about half

that of the first-order reflection from the hexagonal array. The origin of these reflections is not fully understood, though they may arise from either a deformation of the cylindrical microdomains during drying or an inhomogeneous distribution of salt within the microdomains. Fits to the X-ray reflectivity profiles shown in Figure 5c yield the electron density profile shown in Figure 5d, which indicates that there is an electron-dense or a salt-rich region at the interface between the substrate and the copolymer film after drying. In contrast, fits to the reflectivity profiles for the as-cast film show no excess in electron density at the substrate. Consequently, during solvent evaporation, it appears that an excess salt layer forms at the substrate due, more than likely, to an exclusion of excess salt from the ordering front propagating into the film. This can be likened to the exclusion of excess impurities at the ordering front in a zone refinement processes. However, as will be shown later, some of the added salt remains within the PEO cylindrical microdomains. The SFM image in Figure 5e is from a copolymer film with salt ([O]/[K] = 16) that was deposited on silicon substrate having a thick oxide layer. Using a buffered HF solution, the film was removed from the substrate and transferred to a water bath. Subsequently, the film was retrieved on a glass substrate, and part of the film was flipped over onto the transferred film so that both the top and the bottom of the film could be imaged by SFM. While the bottom of the film does not show a change the in orientation of the microdomains, the structure at the bottom of the film is different than that at the top surface. At the bottom, the microdomains are larger and ill defined; however, this is consistent with the destruction of the microdomains and the accumulation of salt during solvent evaporation in copolymer films that contain high amounts of salt.

Cation/anion pairs, other than KI, can be used to complex the PEO block. Figure 6 shows SFM images of different salts that can complex the PEO. LiI ([O]/[Li] = 16), RbI ([O]/[Rb] = 16), and LiCl ([O]/[Li] = 16) shown in parts a, b, and c of Figure 6, respectively, are known to complex PEO while KCl ([O]/[K] = 16), shown in Figure 6d, does not.[42] In cases where the salts complex with the PEO, the cylindrical microdomains orient normal to the surface, while with KCl, the cylindrical microdomains orient parallel to the substrate. Consequently, the specific nature of the salt and its ability to complex with the PEO can be used to effectively tune the orientation of the PEO microdomains.

The addition of a salt to the minor component phase has an added benefit in that the metal ions can be reduced to the corresponding metal, forming nanoscopic metal particles within the block copolymer microdomains. Thus, by default, a controlled placement of metallic nanoparticles in a thin film can readily be achieved. As an example, consider $HAuCl_4$, which is known to complex PEO. Shown in Figure 6e is the TEM image of a copolymer film removed from the substrate after solvent annealing. During the course of the TEM studies, the $HAuCl_4$ was exposed to the electron beam that reduced it to Au, forming Au nanoparticles. It can be seen that the gold nanoparticles (~4 nm in size) formed and were confined within the PEO microdomains. It should be noted that the size of the Au nanoparticles can be controlled by the concentration of gold ions loaded into the films. Similar results were found with Co ions, as shown in Figure 6f, where the cobalt particles are, again, found to be located within the PEO domains. Consequently, the added salt serves a dual role. The first is to orient and order the copolymer microdomains while the second is to serve as a precursor to the fabrication of metal nanoparticles.

Conclusions

We have shown that polymer−salt complexation combined with the solvent annealing affords a simple, yet robust, route to control the orientation and lateral ordering of microdomains in thin films of block copolymer. In addition, the salt can be used as a metal nanoparticle precursor. This strategy is general and can be extended to any block copolymer where one of the components can form a complex with a heavy metal ion salt. Results for PS-*b*-P2VP block copolymers, where the P2VP block can be complexed, shows very similar behavior to that of PS-*b*-PEO. Therefore, this general strategy allows one to generate functional, self-orienting, self-assembling systems that hold promise in the fabrication of nanostructured materials where the spatial placement of each element can be controlled and, as such, opens a pathway to addressable media.

Acknowledgment. We thank Detlef Smilgies for his assistance with the GISAXS measurements at the Cornell High Energy Synchrotron Source. This work was supported by the US Department of Energy, Office of Basic Energy Sciences (DE-FG02-96ER45612 and DE-AC02-98CH10886), and the National Science Foundation sponsored Materials Research Science and Engineering Center at the University of Massachusetts (DMR-0213695).

References and Notes

(1) Hawker, C. J.; Russell, T. P. *MRS Bull.* **2005**, *30*, 952.
(2) Segalman, R. A. *Mater. Sci. Eng., R* **2005**, *48*, 191.
(3) Hamley, I. W. *Nanotechnology* **2003**, *14*, R39.
(4) Lazzari, M.; Lopez-Quintela, M. A. *Adv. Mater.* **2003**, *15*, 1583.
(5) Park, M.; Harrison, C.; Chaikin, P. M.; Register, R. A.; Adamson, D. H. *Science* **1997**, *276*, 1401.
(6) Thurn-Albrecht, T.; Schotter, J.; Kastle, C. A.; Emley, N.; Shibauchi, T.; Krusin-Elbaum, L.; Guarini, K.; Black, C. T.; Tuominen, M. T.; Russell, T. P. *Science* **2000**, *290*, 2126.
(7) Li, R. R.; Dapkus, P. D.; Thompson, M. E.; Jeong, W. G.; Harrison, C.; Chaikin, P. M.; Register, R. A.; Adamson, D. H. *Appl. Phys. Lett.* **2000**, *76*, 1689.
(8) Lopes, W. A.; Jaeger, H. M. *Nature (London)* **2001**, *414*, 735.
(9) Black, C. T.; Guarini, K. W.; Milkove, K. R.; Baker, S. M.; Russell, T. P.; Tuominen, M. T. *Appl. Phys. Lett.* **2001**, *79*, 409.
(10) Cheng, J. Y.; Ross, C. A.; Chan, V. Z. H.; Thomas, E. L.; Lammertink, R. G. H.; Vancso, G. J. *Adv. Mater.* **2001**, *13*, 1174.
(11) Doshi, D. A.; Gibaud, A.; Goletto, V.; Lu, M. C.; Gerung, H.; Ocko, B.; Han, S. M.; Brinker, C. J. *J. Am. Chem. Soc.* **2003**, *125*, 11646.
(12) Ludwigs, S.; Boker, A.; Voronov, A.; Rehse, N.; Magerle, R.; Krausch, G. *Nat. Mater.* **2003**, *2*, 744.
(13) Kim, D. H.; Kim, S. H.; Lavery, K.; Russell, T. P. *Nano Lett.* **2004**, *4*, 1841.
(14) Kim, D. H.; Lau, K. H. A.; Robertson, J. W. F.; Lee, O. J.; Jeong, U.; Lee, J. I.; Hawker, C. J.; Russell, T. P.; Kim, J. K.; Knoll, W. *Adv. Mater.* **2005**, *17*, 2442.
(15) Lin, Y.; Boker, A.; He, J. B.; Sill, K.; Xiang, H. Q.; Abetz, C.; Li, X. F.; Wang, J.; Emrick, T.; Long, S.; Wang, Q.; Balazs, A.; Russell, T. P. *Nature (London)* **2005**, *434*, 55.
(16) Stoykovich, M. P.; Muller, M.; Kim, S. O.; Solak, H. H.; Edwards, E. W.; de Pablo, J. J.; Nealey, P. F. *Science* **2005**, *308*, 1442.
(17) De Rosa, C.; Park, C.; Thomas, E. L.; Lotz, B. *Nature (London)* **2000**, *405*, 433.
(18) Segalman, R. A.; Yokoyama, H.; Kramer, E. J. *Adv. Mater.* **2001**, *13*, 1152.
(19) Segalman, R. A.; Hexemer, A.; Hayward, R. C.; Kramer, E. J. *Macromolecules* **2003**, *36*, 3272.
(20) Harrison, C.; Angelescu, D. E.; Trawick, M.; Cheng, Z. D.; Huse, D. A.; Chaikin, P. M.; Vega, D. A.; Sebastian, J. M.; Register, R. A.; Adamson, D. H. *Europhys. Lett.* **2004**, *67*, 800.
(21) Vega, D. A.; Harrison, C. K.; Angelescu, D. E.; Trawick, M. L.; Huse, D. A.; Chaikin, P. M.; Register, R. A. *Phys. Rev. E* **2005**, 71.
(22) Mansky, P.; Liu, Y.; Huang, E.; Russell, T. P.; Hawker, C. *Science* **1997**, *275*, 1458.
(23) Ryu, D. Y.; Shin, K.; Drockenmuller, E.; Hawker, C. J.; Russell, T. P. *Science* **2005**, *308*, 236.
(24) Thurn-Albrecht, T.; DeRouchey, J.; Russell, T. P.; Jaeger, H. M.; *Macromolecules* **2000**, *33*, 3250.

(25) DeRouchey, J.; Thurn-Albrecht, T.; Russell, T. P.; Kolb, R. *Macromolecules* **2004**, *37*, 2538.
(26) Kim, G.; Libera, M. *Macromolecules* **1998**, *31*, 2569.
(27) Kim, S. H.; Misner, M. J.; Xu, T.; Kimura, M.; Russell, T. P. *Adv. Mater.* **2004**, *16*, 226.
(28) Bruce, P. G. *Chem. Commun.* **1997**, 1817.
(29) MacGlashan, G. S.; Andreev, Y. G.; Bruce, P. G. *Nature (London)* **1999**, *398*, 792.
(30) Andreev, Y. G.; Bruce, P. G. *Electrochim. Acta* **2000**, *45*, 1417.
(31) Gadjourova, Z.; Andreev, Y. G.; Tunstall, D. P.; Bruce, P. G. *Nature (London)* **2001**, *412*, 520.
(32) Tarascon, J. M.; Armand, M. *Nature (London)* **2001**, *414*, 359.
(33) Pereira, R. P.; Rocco, A. M.; Bielschowsky, C. E. *J. Phys. Chem. B* **2004**, *108*, 12677.
(34) Christie, A. M.; Lilley, S. J.; Staunton, E.; Andreev, Y. G.; Bruce, P. G. *Nature (London)* **2005**, *433*, 50.
(35) Ruzette, A. V.; Soo, P. P.; Sadoway, D. R.; Mayes, A. M. *J. Electrochem. Soc.* **2001**, *148*, A537.
(36) Spatz, J. P.; Herzog, T.; Mossmer, S.; Ziemann, P.; Moller, M. *Adv. Mater.* **1999**, *11*, 149.
(37) Breulmann, M.; Forster, S.; Antonietti, M. *Macromol. Chem. Phys.* **2000**, *201*, 204.
(38) Sohn, B. H.; Yoo, S. I.; Seo, B. W.; Yun, S. H.; Park, S. M. *J. Am. Chem. Soc.* **2001**, *123*, 12734.
(39) Glass, R.; Moller, M.; Spatz, J. P. *Nanotechnology* **2003**, *14*, 1153.
(40) Renaud, G.; Lazzari, R.; Revenant, C.; Barbier, A.; Noblet, M.; Ulrich, O.; Leroy, F.; Jupille, J.; Borensztein, Y.; Henry, C. R.; Deville, J. P.; Scheurer, F.; Mane-Mane, J.; Fruchart, O. *Science* **2003**, *300*, 1416.
(41) Dourdain, S.; Rezaire, A.; Mehdi, A.; Ocko, B. M.; Gibaud, A. *Phys. Rev. B: Condens. Matter* **2005**, *357*, 180.
(42) Ratner, M. A.; Shriver, D. F. *Chem. Rev.* **1988**, *88*, 109.

MA061170K